Ultraviolet photorefraction and the superionic phase transition of α-LiIO$_3$

Jingjun Xu, Xuefeng Yue, and Romano A. Rupp

Fachbereich Physik, Universität Osnabrück, 49069 Osnabrück, Germany

(Received 20 June 1996; revised manuscript received 16 August 1996)

The photorefractive effect is investigated in nominally pure α-LiIO$_3$ crystals within the 333–514.5 nm spectral range. In the temperature range of 180 K–240 K, i.e., the temperature range of the superionic phase transition, a dramatic decrease of the diffraction efficiency by a factor 100 is observed. This can be explained by the formation of an ionic complementary grating having an activation energy for thermal erasure of 0.32 ± 0.03 eV. Thermal fixing can be achieved by holographic recording at temperatures below about 180 K, developing the complementary grating at room temperatures, and finally recovering the complementary grating below 180 K. In contrast to the assumptions made for the thermal fixing process in other crystals, e.g., LiNbO$_3$, the mobile ionic species in α-LiIO$_3$ are mainly lithium ions. [S0163-1829(96)06147-4]

I. INTRODUCTION

The photorefractive effect arises under nonuniform illumination from a charge redistribution which causes a change of the refractive index by the electro-optic effect. Because of potential applications of photorefractive materials in real-time holography, image processing, light amplification, optical phase conjugation, and nonlinear optics, the interest in this field has considerably grown in the last few years.[1] The main effort has been focused on materials that are photosensitive in the visible or near-infrared spectral range. Photorefractive materials working in the ultraviolet (UV), however, are needed for all coherent optical beam interactions in which improved resolution and storage capacity are required. Until now, only preliminary studies of the photorefractive effect in the UV have been reported, for example, in KH$_2$PO$_4$, RbZnBr$_4$, LiNbO$_3$, LiTaO$_3$, Bi$_4$Ge$_3$O$_{12}$, and doped LiIO$_3$.[2–8]

Lithium iodate crystals of hexagonal modification (α-LiIO$_3$) have been investigated in detail as the first quasi-one-dimensional ionic conductors.[9] A number of novel phenomena were discovered in this material. Among them, the wide-angle light diffraction band is the most interesting one, which is analogous to the photorefractive effect.[9] Fluctuations of interstitial ions and/or ion vacancies are responsible for this kind of light scattering while electrons and/or holes are responsible for the photorefractive effect. A strong photorefractive effect is expected in α-LiIO$_3$, because it exhibits large electrooptic coefficients. However, until now only a few studies on photorefraction of α-LiIO$_3$ have been undertaken. In 1983, the photorefractive effect in doped α-LiIO$_3$ was first observed by Pogosyan *et al.*[7] by measuring the light-induced change of the birefringence, and it was pointed out that the photovoltaic effect was not the reason for the photorefractive effect. In 1995, Laeri *et al.*[8] reported on their observations of photorefraction in doped α-LiIO$_3$ by the holographic recording method. They found that the PR effect was strongly dependent on doping in the crystal. Energy transfer by two-wave mixing was neither found in doped nor in undoped ones. The mechanism for the photorefractive effect in lithium iodate crystals remained still in doubt.

In this paper we report our investigations on photorefrac-tion in nominally pure α-LiIO$_3$ within the spectral range (333–514.5 nm) and a wide temperature range (90–290 K). We found that the photorefractive properties of nominally pure α-LiIO$_3$ crystals have a close relationship with the superionic phase transition.

II. EXPERIMENTAL DETAILS

A sample with linear dimensions of $12 \times 4 \times 5$ mm^3 was cut along the a,b,c crystallographic axes from a nominally pure lithium iodate crystal. This sample was already used by Zhang *et al.* to study light scattering.[10] As the absorption measurement shows, the sample has very small absorption from 320 nm to 600 nm (Fig. 1), which is suitable for us to investigate photorefraction in the ultraviolet spectral region down to 333 nm. This is, as a rule, not possible with doped samples.

The direction of the c axis was determined by the static piezoelectric effect. According to the international convention, the outwardly drawn normal to the c surface, which becomes positively charged under tensile stress, is the $+c$
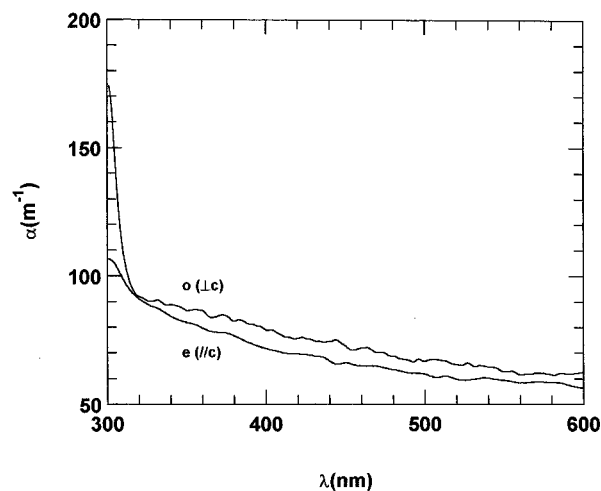

FIG. 1. Absorption spectra for nominally pure α-LiIO$_3$ at room temperature. Reflection losses were taken into account, but light scattering not.

    <u>54</u>   16 618

direction. For this purpose, silver electrodes were painted on the c surfaces of the sample. The sample was placed into a screening cell with c surfaces contacting the cover and bottom of the cell. They served as electrodes and were connected to an electroscope. By pressing and unpressing the cover to change the tensile stress on the sample, we determined the signs of the charges on the c surfaces.

We performed our experiments using the traditional setup for holographic recording. The grating vector was oriented along the c axis of the crystal. The hologram was written by two Ar$^+$ laser beams (333 nm–514.5 nm) and read out with a weak He-Ne laser beam (632.8 nm) or one of the writing beams incident under the Bragg angle. The diffraction efficiency η was defined as

$$\eta = I^d/(I^d + I^t),$$

where I^d is the diffracted and I^t the transmitted light intensity. The two-wave coupling gain was defined as

$$\Gamma = (1/l_{\text{eff}})\ln(I^p/I^s),$$

where l_{eff} was the effective interaction length,[11] $l_{\text{eff}} = d[1 - \exp(-D/d \sin 2\theta_i)]$ (d is the thickness (4 mm) of the sample, D the diameter (2.5 mm) of the light beam, $2\theta_i$ is the intersection angle between two recording beams in the crystal); I^p and I^s are the transmitted signal intensities with and without incidence of the pump light on the crystal, respectively.

In the setup, a Soleil-Babinet compensator was used to change the polarization of the incident light. In our experiment, the polarization of the erasing light was always adjusted to be perpendicular to that of the writing light.

The temperature dependence of photorefraction was studied by placing the crystal in a liquid-nitrogen cryostat in a static vacuum of about 10^{-4} Torr. This avoided spurious changes in the optical paths produced by thermal convection. The temperature was measured with a nickel-chromium thermocouple attached to the sample holder. At room temperature, the sample was placed directly on the sample flat without the cryostat, so that the measurement could be carried out for a large range of the intersection angle 2θ.

III. ULTRAVIOLET PHOTOREFRACTION IN NOMINALLY PURE α-LiIO$_3$ AT ROOM TEMPERATURE

To study the photorefractive behavior in nominally pure α-LiIO$_3$, we performed holographic recording experiments and light amplification experiments by two-wave mixing with a laser intensity between 2.5 W/cm^2 and 50 W/cm^2 within the wavelength range of 333–514.5 nm. In the experiments extraordinary polarization and a grating vector parallel
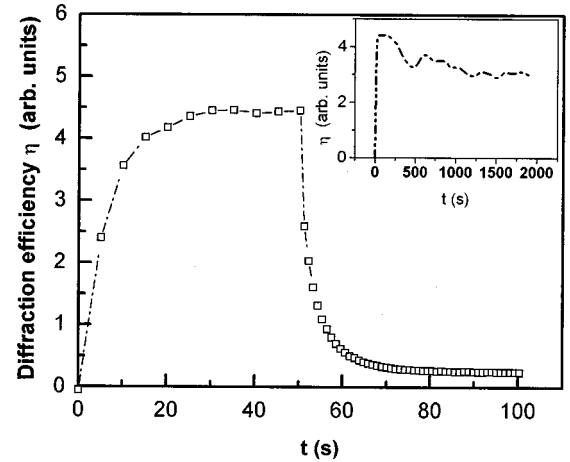

FIG. 2. Holographic recording and optical erasure cycle with the same intensity, 18 W/cm^2 in each writing beam at an external intersection angle $2\theta = 60°$ for a wavelength $\lambda = 351$ nm and for room temperature. Inset: Long-time behavior of holographic recording.

to the crystal c axis were chosen to use the electrooptical tensor coefficient r_{33} of the α-LiIO$_3$ crystal.

Figure 2 shows the holographic recording and optical erasure cycle at room temperature and for an incident light intensity of 18 W/cm^2 in each writing beam. Holographic recording on a larger time scale is also shown in the inset of Fig. 2. For long-time recording, the diffraction efficiency decreases slowly with increasing recording time. Holographic gratings could be recorded in our sample throughout the laser wavelength range of 333–514.5 nm as shown in Table I.

The light-induced refractive-index amplitude Δn was calculated from the diffraction efficiency η with

$$\eta = \sin^2[\pi \Delta n d/(\lambda \cos\theta_r)], \qquad (1)$$

assuming that a phase grating is the dominant contribution to photorefraction in our case (Table I). Here λ is the free space wavelength and θ_r the Bragg angle of the readout beam in the crystal. Using Eq. (1), we estimated the light-induced refractive-index change in the sample as shown in Table I. For an external intersection angle $2\theta = 60°$ and an intensity of 18 W/cm^2 in each writing beam, the maximum light-induced refractive-index change $\Delta n_{\max} \sim 8.9 \times 10^{-7}$ occurred at 333 nm.

The maximum diffraction efficiencies of the holographic gratings were almost the same within the range of the working intensity 2.5 W/cm^2–50 W/cm^2, as shown in Fig. 3. This is one of the characteristics of the photorefractive effect for the case that the ratio of the dark conductivity σ_D to the photoconductivity σ_{ph} fulfills $\sigma_D/\sigma_{\text{ph}} \ll 1$.

TABLE I. Maximum diffraction efficiencies $\eta_{\max}$ and refractive index amplitudes Δn of photorefractive gratings in nominally pure α-LiIO$_3$ at different laser wavelengths λ. Experimental conditions: room temperature, $2\theta = 60°$, intensity 18 W/cm^2 in each writing beam, grating vector oriented along the c axis of the crystal, one of the writing beams used as a readout beam.

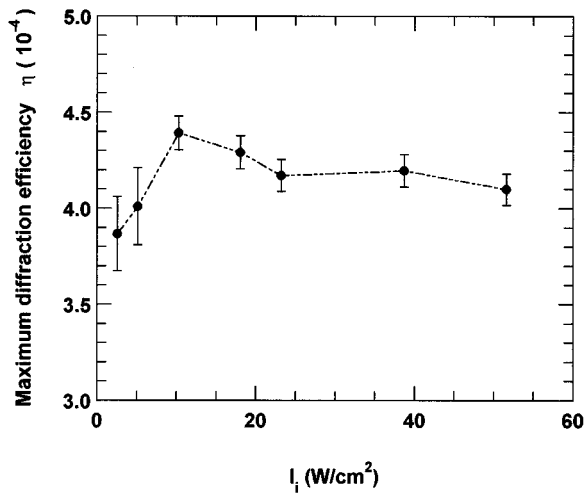| λ (nm)	333	351	364	457	488	515
$\eta_{\max}$ (%)	0.12	0.045	0.02	$\sim 5 \times 10^{-3}$	$\sim 10^{-3}$	$\sim 10^{-3}$
Δn ($\times 10^{-7}$)	8.9	5.7	4.0	~ 2.5	~ 1.2	~ 1.2

FIG. 3. Dependence of the maximum diffraction efficiency η_{max} on the incident light intensity I_i. (Experimental conditions are the same as in Fig. 2.)

If we recorded the grating for a long time, e.g., for more than half an hour and started to erase the grating by illumination with a laser beam, we observed an optical erasure process similar to that reported in Ref. 8, which is shown in Fig. 4. This result suggests that another complementary grating was formed in the crystal to compensate the primary grating. This suggestion is also in agreement with the experimental results of the long-time recording as shown in the inset of Fig. 2. We use the equation

$$\eta = \eta_0 [\exp(-t/\tau_1) - W \exp(-t/\tau_2)]^2$$

to fit the results in Fig. 4 and get 12 s and 480 s, respectively, for the time constants τ_1 and τ_2 of the two processes and 0.15 for W, 6×10^{-4} for η_0.

Energy transfer by two-wave mixing was also observed in this kind of crystal as shown in Fig. 5. Energy was always
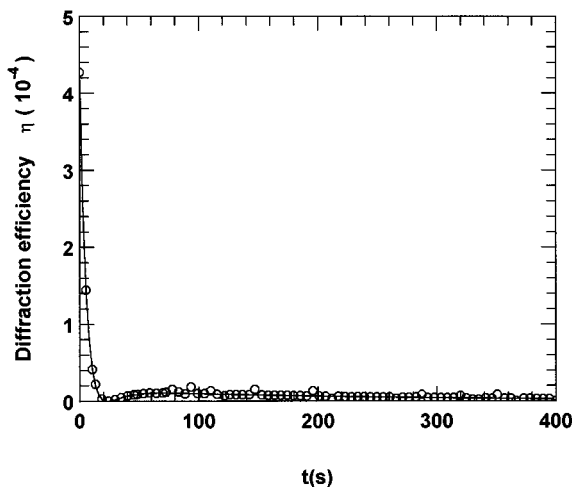

FIG. 4. Optical erasure of the grating recorded for a long time, e.g., for more than half an hour. (Experimental conditions are the same as in Fig. 2.) The solid line is a theoretical fit according to the equation $\eta = \eta_0 [\exp(-t/\tau_1) - W \exp(-t/\tau_2)]^2$, where η_0, τ_1, τ_2, and W are fitting parameters.
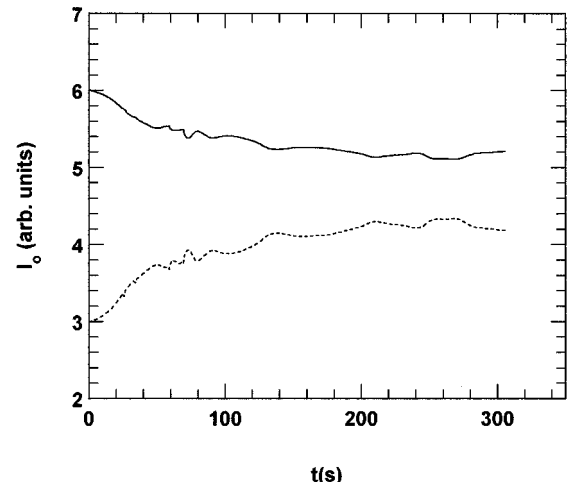

FIG. 5. Two-wave mixing ($2\theta = 60°$, $\lambda = 351$ nm, pump-signal ratio $r = 10$). The dashed line corresponds to the signal light while the solid one corresponds to the pump light.

transferred to the beam in the direction of the negative c axis of the crystal. The direction of energy transfer by two-wave mixing was the same for the case of the two writing beams with ordinary polarizations. This kind of the asymmetric energy transfer between two writing beams is one of the main characteristics of the photorefractive effect, which distinguishes photorefractive gratings from other kinds of gratings, for example, absorption gratings, which can only cause symmetric energy transfer, namely, simultaneous increase or decrease of the intensities of both beams.

We determined the sign of the majority charge carriers using two-wave mixing configuration with two ordinarily polarized writing beams, thereby the electrooptic coefficient r_{13} is utilized. We use a Michelson interferometer setup with an Ar$^+$ laser as monochromatic source to determine the sign of r_{13}. A glass plate and the sample with its c axis perpendicular to both optical path and the light polarization were both inserted to one of the two optical paths between the beamsplitter and the mirrors. An external electric field E_{ex} was applied to the sample parallel to the c axis and induced a change Δn of the refractive index of the sample. As a result of the change of the refractive index, the light interference pattern moved. By rotating the glass plate, we concluded that the direction of motion of light interference pattern induced by the application of the external electric field on the sample was due to a decrease of the refractive index of the sample. So we determined the sign of the linear electrooptic coefficient r_{13} to be positive in our sample using the relationship of $\Delta n \propto -r_{13}E_{ex}$. Based on the experimental results of $r_{13} > 0$ and $\Gamma < 0$ (energy is always transferred to the beam in the direction of the negative c axis of the crystal) we conclude that electrons are the dominant charge carriers responsible for two-wave mixing in our sample.

Figure 6 shows two-wave mixing on a larger time scale. The two-wave coupling gradually became weaker, which might be caused by complementary gratings compensating the primary one, in agreement with the interpretation given for the result of the diffraction efficiency measurements (Fig. 2 and Fig. 4).
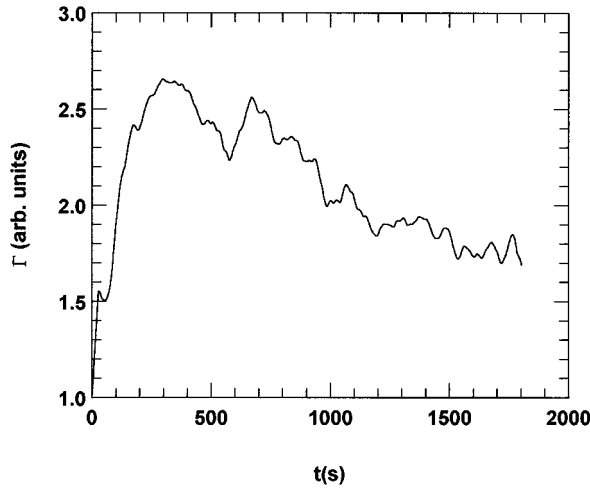
FIG. 6. Long-time behavior of two-wave mixing ($2\theta=60°$, $\lambda=351$ nm, pump-signal ratio $r=10$).

IV. THERMAL FIXING AND RELATED THERMAL EFFECTS

In our study on the temperature dependence of photorefracive gratings, laser light with the wavelength of 333 nm was used, and the intersection angle 2θ of both writing beams was kept at 14°. The maximum diffraction efficiencies of the photorefractive gratings recorded at different temperatures are shown in Fig. 7. On cooling down from room temperature, the diffraction efficiency increases at first only slowly with temperature. At 240 K the diffraction efficiency begins to rise dramatically with decreasing temperature until down to about 180 K where a maximum as high as 2% is achieved, which is more than 100 times higher than the values for room temperature. For lower temperatures the diffraction efficiency slightly decreases. We also measured the temperature dependence of the two-wave-coupling gain, and found that the gain also increased by a factor of about 6 with decreasing temperature.

For the light-induced refractive index change we have

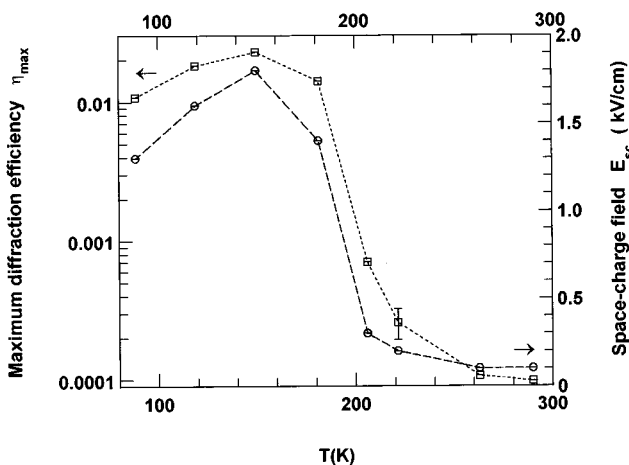$$\Delta n = -\tfrac{1}{2}n^3 r_{\mathrm{eff}} E_{\mathrm{sc}}, \qquad (2)$$

FIG. 7. Dependence of the maximum diffraction efficiency $\eta_{\max}$ and the light-induced space-charge field E_{sc} on the temperature of the sample ($2\theta=14°$, $\lambda=333$ nm).
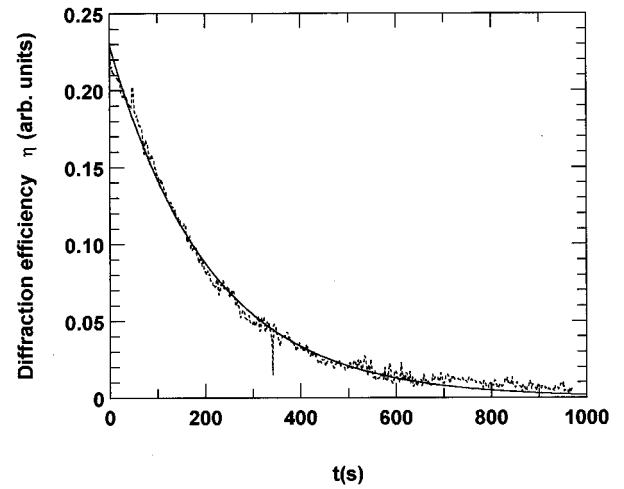

FIG. 8. Optical erasure of a grating recorded at the temperature of 100 K. The solid line is a theoretical fit according to the equation $\eta=\eta_0\exp(-2t/\tau)$ and the dashed one is the experimental result ($I_i=18$ W/cm^2, $2\theta=14°$, $\lambda=333$ nm).

where n is the effective refractive index. For our chosen geometry—conventional symmetrical configuration, we have $n=n_e n_o/(n_e^2\sin^2\theta_i+n_o^2\cos^2\theta_i)^{1/2}$ for the two writing beams with e polarizations and $n=n_o$ for the two writing beams with o polarizations.

Here r_{eff} is the effective electro-optic coefficient, $r_{\mathrm{eff}}=(n_e^4 r_{33}\cos^2\theta_i-n_o^4 r_{13}\sin^2\theta_i)/n^4$ for e-polarized writing beams and $r_{\mathrm{eff}}=r_{13}$ for o-polarized writing beams. Using Eqs. (1) and (2) with $n_e=1.8134$, $n_o=1.9874$, $r_{13}=4.1$ pm/V, $r_{33}=6.4$ pm/V, and the experimental results in Fig. 7, we calculated the light-induced space-charge field formed in the crystal at different temperatures, which is also shown in Fig. 7.

Figure 8 shows the optical erasure of a grating which had been recorded at 100 K. The erasure process was monoexponential with a time constant of 416 s, obtained from fitting the function $\eta=\eta_0\exp(-2t/\tau)$ to the results. No matter how long we recorded, there was only one decay constant. This behavior of optical erasure is different from that at room temperature where we could distinguish two time constants, which shows that the complementary grating, occurring at room temperature, is suppressed at low temperatures.

We successfully fixed the complementary gratings, using the following technique: First we recorded the gratings at low temperature T_l. After reaching the maximum diffraction efficiency both writing beams were blocked. Then we increased the temperature up to T_d, keeping the sample at this temperature until the gratings completely decayed away. Subsequently, we decreased the temperature to T_f, where the sample was illuminated with one erasure beam. During the whole process, a weak He-Ne laser beam (632.8 nm) adjusted at the Bragg angle detected the change of the diffraction efficiency of the grating.

Figure 9 shows a record of the sequence performed to fix the complementary grating at low temperature: First a photorefractive grating with a diffraction efficiency of 1.1% was recorded at $T_l=90$ K. Then the sample temperature was increased at an average heating speed of about 6.0 K/min while both writing beams were blocked (A). Starting from
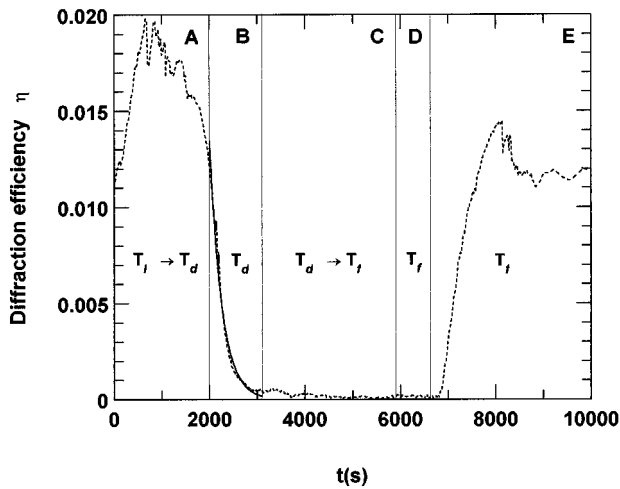
FIG. 9. Process of thermal fixing. Region A, both writing beams are blocked and the temperature increases from 90 K to 290 K; region B, both writing beams are blocked and the temperature is kept at 290 K; region C, both writing beams are blocked and the temperature decreases from 290 K to 90 K; region D, both writing beams are blocked and the temperature is kept at 90 K; region E, the temperature is kept at 90 K, one of the beams illuminates the sample. The solid line in the region B is a theoretical fit according to the equation $\eta = \eta_0 \exp(-2t/\tau)$ ($2\theta = 14°$, $\lambda = 333$ nm).

90 K to 150 K the diffraction efficiency increased from 1.25% to 2.1%, and then began to decrease while the temperature was raised further to $T_d = 290$ K. Keeping the temperature at 290 K we could see that the grating gradually decayed away (B). By fitting the result with the equation $\eta = \eta_0 \exp(-2t/\tau)$, we got a decay time constant of about 508 s. After complete decay of the gratings, we cooled the sample again down to $T_f = 90$ K with an average cooling speed of about 3.3 K/min (C). At this temperature, no light diffraction was observed (D). We began to illuminate the sample with a laser beam of polarization perpendicular to the former recording beams (E). The diffracted light appeared quickly, increased to a maximum diffraction efficiency as high as 1.5% followed by a slight decrease. Finally a steady-state value was reached. The grating in the sample could not be erased by illumination of the laser light. This means that we finished with a thermally fixed complementary grating in the sample.

We measured the thermal erasure of the fixed grating by annealing it at a temperature T_d. Our experimental results reveal that the complementary gratings are completely frozen at temperatures below about 180 K. From about 180 K on the grating began to decay, but the decay rate at temperatures below 220 K is still so slow that we could not determine the exact time constant. So here we only gave our results between 240 K and 290 K, which are shown in Fig. 10.

V. DISCUSSION

From our above experimental results we found that a complementary grating is formed in the crystal at room temperature and can be frozen in below 180 K (thermal fixing). The following arguments suggest that it originates from mobile ions.
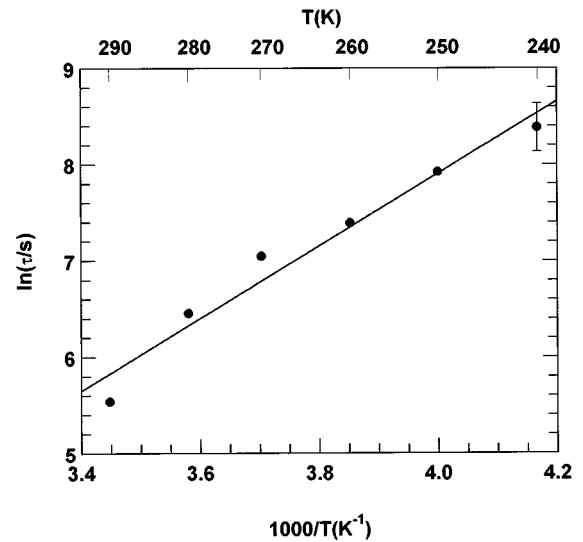

FIG. 10. Dependence of the dark decay time constant τ of the complementary grating on the temperature. The solid straight line is a theoretical fit according to the equation $\tau = \tau_0 \exp(E_0/K_B T)$ ($2\theta = 14°$, $\lambda = 333$ nm, $I_i = 18$ W/cm^2).

(i) In α-LiIO$_3$ crystals, the lithium ions are in an octahedral environment of oxygen ions. The voids of these octahedra are joined by their faces, forming channels along the c axis of the crystal. The interstitial ions and/or ion vacancies can move quite freely along these channels, because the energy needed for the transfer of interstitial ions and/or ion vacancies from their equilibrium positions to vacant adjoining ones is relatively low (0.3–0.6 eV).[9,12–14] We also measured the absorption spectrum in the infrared range (2000–5000 cm^{-1}) shown in Fig. 11. Absorption bands within the wave-number range between 3200 cm^{-1} and 3600 cm^{-1}, similar to those reported in Ref. 15, show that H$^+$ ions exist in the crystals, too. Like in LiNbO$_3$ crystals, these H$^+$ ions possibly contribute in addition to the interstitial Li$^+$ and/or Li$^+$ vacancies to the ionic migration in the crystal. In addition, the light-induced space-charge field in the crystal could
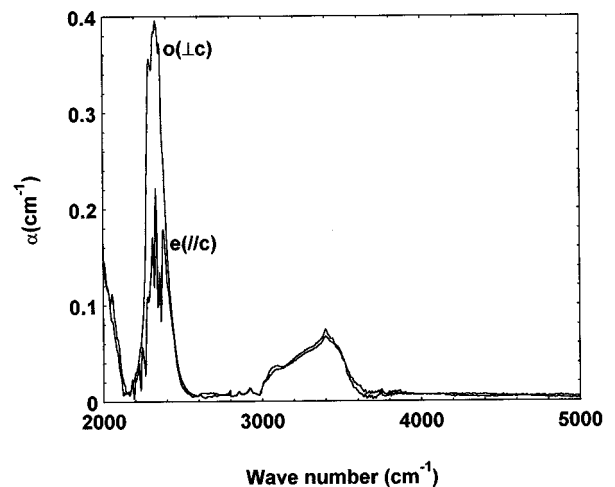

FIG. 11. Infrared absorption spectrum for the nominally pure α-LiIO$_3$ used in our experiments.

reach to as high as about 1.8 kV/cm as shown in Fig. 7. So under this light-induced space-charge field, it is clear that these ions move along the c axis and compensate the primary light-induced space-charge field.

(ii) For a single thermally activated process contributing to the decays, the characteristic decay time constant τ, depends on the sample temperature as $\tau = \tau_0 \exp(E_0/K_B T)$, where τ_0 is a preexponential time factor, and E_0 the activation energy of the process responsible for thermal erasure. In Fig. 10, we use a logarithmic plot of the dark decay time constant τ versus $1000/T$ to fit the experimental results. From the slope of the fitted line we obtain an activation energy $E_0 \sim 0.32 \pm 0.03$ eV. This value is in agreement with the activation energy for the migration of lithium ions obtained by measuring the temperature dependence of the ionic conductivity.[12,14]

(iii) From the above experimental results we see that the complementary gratings are frozen at temperatures below 180 K. This temperature limit is the same as the one freezing the ions in neutron scattering experiments and in investigations of the wide-angle light diffraction band.[9]

(iv) Nearly the same decay time constants of the complementary grating were measured for optical (480 s) and thermal erasure (508 s). This is to be expected, because the complementary gratings should be insensitive to the illumination of the laser light. The same characteristics were observed before for the noise gratings formed in nominally pure α-LiIO$_3$ crystals by ions under externally applied electric field.[9,16]

From the above discussions, we can see that ions play an important role in the photorefractive effect of the crystal, and are responsible for the complementary grating.

Next let us consider the primary grating formed in the crystal. Vacancies and impurities are commonly present even though the crystal is grown without doping. These impurities could work as donors and acceptors for the charge carriers to form the primary grating. In addition, the experiments were mostly performed at laser wavelengths near the intrinsic absorption band (as shown in Fig. 1), so that the intrinsic band structure might also participate in the photorefractive effect.

From the experimental results of Fig. 5, we know that diffusion is the dominant mechanism for the photorefractive effect. So the light-induced space-charge field is given by $E_{sc} \propto E_D$ ($\propto T$) ($E_D = K k_B T/q$ is the diffusion field, K is the magnitude of the grating vector, k_B is Boltzmann constant, q is the carrier charge). The experimental results of Fig. 7 within the temperature range of 90 K–150 K are in good agreement with the relationship of $E_{sc} \propto T$. However, the light-induced space-charge field decreases dramatically while the temperature increases from 180 K to 240 K. This is not to be expected by the present theory on the photorefractive effect. So other unknown mechanisms or processes exist in our sample, which is identified to be the superionic phase transition in α-LiIO$_3$ reported in Ref. 12 at the critical temperature $T_C = 243$ K. In α-LiIO$_3$ the process of Li$^+$-ion disordering starts from 170 K to 180 K. With increasing temperature the Li$^+$-ion disordering achieves a high degree. The high degree of the process of Li sublattice disordering causes abnormally high values of the dielectric permeability by means of thermal ion polarization. If the temperature is raised to 243 K, the high degree of Li$^+$ ion

disordering along with the high dielectric permeability and electroconductivity leads to the collective interaction of the whole set of disordered ions and vacancies left by them to form a united conglomerate — the superionic state. In our experiment, it was also found that at $T \sim 180$ K the diffraction efficiency begins to change dramatically within the temperature range of 180 K–240 K, which is exactly the same as the region of the ion disordering. This suggests that the superionic phase transition contributes decisively to the dramatic change of the diffraction efficiencies within the temperature range of 180 K–240 K. If so, holographic experiments provide a method to study the superionic phase transition.

In addition, some effects may also be related to the photoreactive effect in the crystal, for example, photovoltaic effect, pyroelectric effect, piezoelectric effect, etc.,[7,9,17–20] and all of these effects change a great deal with the change of the sample temperature. It is relatively complicated to analyze them, because these effects can influence the photorefractive effect altogether. Fortunately, all of the above effects change in nominally pure α-LiIO$_3$ crystals not as greatly as in doped ones. So it should be easier to study it in nominally pure α-LiIO$_3$ crystals than in doped ones.

VI. CONCLUDING REMARKS

We have recently repeated the above experiments in several other nominally pure α-LiIO$_3$ crystals, and found that they exhibit the same photorefractive behaviors as described here. The results reveal that cooling below the temperature of the superionic phase transition can definitely be utilized to get phase gratings of high diffraction efficiency and to effectively fix the complementary gratings; on the other hand, holographic experiments also provide an effective method to study the superionic phase transition in solid-state ionic conductors.

In nominally pure α-LiIO$_3$ crystals, there are few photo-induced electric charges. This limits the formation of strong light-induced space-charge electric field, so it may be expected that the diffraction efficiency of the phase gratings can be increased by increasing the density of the photoinduced electric charges in suitably doped crystals.

The ease of thermal fixing in α-LiIO$_3$ crystals and other solid-state ionic conductors and the large diffraction efficiencies obtained by thermally fixed ionic gratings make these materials one of the most promising candidates for neutron scattering[21] and other similar applications.

ACKNOWLEDGMENTS

[1] For an overview see *Photorefractive Materials and Their Applications*, edited by P. Günter and J. Huignard (Springer-Verlag, Berlin, 1988, 1989), Vols. I and II.

[2] V. M. Fridkin, B. N. Popov, and K. A. Verkhovskaya, Appl. Phys. **16**, 313 (1978).

[3] T. Nakamura, V. M. Fridkin, R. Magomadov, M. Takashhige, and K. Verkhovskaya, J. Phys. Soc. Jpn. **48**, 1588 (1980).

[4] R. Orlowski, E. Krätzig, and H. Kurz, Opt. Commun. **20**, 171 (1977).

[5] E. Krätzig and R. Orlowski, Appl. Phys. **15**, 133 (1978).

[6] G. Montemezzani, St. Pfändler, and P. Günter, J. Opt. Soc. Am. B **9**, 1110 (1992).

[7] A. R. Pogosyan, E. M. Uyukin, and G. F. Dobrzhanskii, Sov. Phys. Solid State **24**, 2063 (1982).

[8] F. Laeri, R. Jungen, G. Angelow, U. Vietze, T. Engel, M. Würzt, and D. Hilgenberg, Appl. Phys. B **61**, 351 (1995).

[9] Xu Zheng-Yi, Prog. Phys. **9**, 17 (1989).

[10] G. Y. Zhang, J. Liu, and S. T. Feng, Acta Phys. Sin. **33**, 710 (1984).

[11] G. C. Valley, J. Opt. Soc. Am. B **4**, 14 (1987).

[12] A. E. Aliev, A. Sh. Akramov, L. N. Fershtat, and P. K. Khabibullaev, Phys. Status Solidi A **108**, 189 (1988).

[13] Y. Zhu, D. F. Zhang, and X. M. Feng, Acta Phys. Sin. **26**, 115 (1977).

[14] B. V. Shchepetil'nikov, A. I. Baranov, and L. A. Shuvalov, Sov. Phys. Solid State **29**, 450 (1987).

[15] Lawrence S. Goldberg, Appl. Opt. **14**, 653 (1975).

[16] Yin-Yuan Li, Solid State Ion. **31**, 99 (1988).

[17] A. S. Bhalia, J. Appl. Phys. **55**, 1229 (1984).

[18] Kh. S. Bagdasarov, V. F. Karyagin, A. R. Pogosyan, and E. M. Uyukin, Sov. Phys. Solid State **25**, 1043 (1983).

[19] A. R. Pogosyan, E. M. Uyukin, A. P. Levanyuk, and G. F. Dobrzhanskii, Sov. Phys. Solid State **23**, 1906 (1981).

[20] M. Szafranski, Solid State Commun. **75**, 535 (1990).

[21] R. A. Rupp, Opt. Mater. **4**, 276 (1995).